Systems & Control Transactions

Research Article - Peer Reviewed Conference Proceeding
ESCAPE 35 - European Symposium on Computer Aided Process Engineering
Ghent, Belgium. 6-9 July 2025
Jan F.M. Van Impe, Grégoire Léonard, Satyajeet S. Bhonsale,
Monika E. Polańska, Filip Logist (Eds.)

PSE PRESS

Development of a virtual CFD model for regulating temperature in a liquid tank

Jinxin Wang[a], Feng Xu[a], Yuka Sakai[a], Hisashi Takahashi[b], Ruizi Zhang[c], Hiroaki Kanayama[c], Daisuke Satou[c], Yasuki Kansha[a,c]*

[a] Organization for Programs on Environmental Sciences, Graduate School of Arts and Sciences, The University of Tokyo, 3-8-1 Komaba, Meguro-ku, Tokyo 153-8902, Japan
[b] TechnoPro, Inc. TechnoPro R&D Company, Roppongi Hills Mori Tower 35F, 6-10-1 Roppongi, Minato-ku, Tokyo 106-6135, Japan
[c] Technology and Innovation Center, Daikin Industries, LTD., 1-1 Nishi-Hitotsuya, Settsu, Osaka 566-8585, Japan
* Corresponding Author: kansha@global.c.u-tokyo.ac.jp

ABSTRACT

Temperature regulating in liquid tanks is critical in the chemical industry and conventionally relies on sensor feedback. However, due to the complex thermo-hydrodynamics, unsensed local temperatures can deviate from desired thresholds, underscoring the need for improved tank temperature modeling. The absence of internal thermal or flow data, however, poses significant challenges for the development and validation of effective control strategies. In this study, a virtual model for regulating liquid tank temperature was developed using computational fluid dynamics (CFD). Adaptions were made mainly by involving (1) a simple on-off mechanism of feeding based on a virtual sensor to achieve temperature within the acceptable range and (2) the imposition of unfavorable temperatures on the walls representing ambient influences. Leveraging this virtual system, several new cases were simulated. The simulation results highlighted pronounced temperature non-uniformity, with discrepancies exceeding 2°C between sensor readings and interior points, even leading to inefficiencies of regulatory mechanism. Additionally, the buoyancy was found to significantly influence the internal thermal distributions, and proper outlet position can help alleviate the temperature non-uniformity. Thus, the proposed CFD model serves as a reliable platform for generating comprehensive datasets to support temperature regulation studies in liquid tanks.

Keywords: Liquid tank, temperature regulating, CFD, thermal non-uniformity, stratification, buoyancy.

INTRODUCTION

Liquid temperature non-uniformity is a widespread issue in the chemical industry and thermal management. For instance, maintaining minimal temperature differences within materials should be crucial, as emphasized by the pharmaceutical and food industries, which prioritize thermal uniformity during heating processes [1,2]. Moreover, uneven temperature distribution can cause discomfort for living beings in facilities such as public baths and aquariums.

However, it is impractical to install many physical sensors in the above facilities to measure local temperatures, and current temperature regulation systems often assume uniformity within the unit [3,4]. It is well-established that density variations caused by temperature differences can result in thermal stratification, where buoyancy drives less dense fluid upward. Consequently, sensed temperatures often deviate from actual internal values, leading to less effective control. Fortunately, recent studies have begun addressing this issue through soft-sensor development. Experimental research involving local temperature measurements and flow field visualization has been conducted [4,5]. However, experiments are labor-cost and limited by the availability of facilities.

Computational fluid dynamics (CFD) offers a powerful alternative by providing detailed internal temperature distributions to inform regulation systems. CFD excels at handling complex thermo-hydrodynamics by solving the

Navier-Stokes equations coupled with the energy equation. Control-integrated CFD models have been employed for over a decade to optimize air-conditioning control strategies, despite concerns about computational cost [6]. More recently, CFD has been combined with deep learning frameworks for indoor environmental control [7]. With advancements in computational hardware, CFD is poised to play an increasingly significant role in developing temperature regulation systems.

However, CFD is still underutilized for liquid temperature regulation. A CFD-based model can facilitate system design refinement with quantified insights into thermal field distributions but requires a highly adaptive interface for diverse industrial scenarios and considerable computational resources. Recently, water stratification was investigated thoroughly for energy storage, taking up to 18 days of computation per case [8]. Over the past decade, the open-source CFD software OpenFOAM has gained traction due to its fully adaptable framework, making it a valuable tool for customizing industrial processes. With the rapid expansion of data centers, advancing CFD-based temperature regulation becomes increasingly essential for improving product quality and energy efficiency in industries.

This study aims to bridge the above research gap by introducing the CFD method into the investigation of liquid temperature regulation in a tank. An original CFD model was developed using the OpenFOAM framework and validated against experimental data. The model was adapted as a virtual temperature regulation system, involving ambient temperature influences and integrated with a simple on-off control mechanism. Several regulation scenarios via heating and cooling were simulated and analyzed. The results demonstrated that thermal non-uniformity was well captured, revealing severe temperature discrepancies between interior locations and the virtual sensor. These discrepancies can even disable the regulatory mechanism under severe stratification conditions. The effects of outlet and sensor positions were also investigated in cooling scenarios. Our model enables an in-depth analysis of thermal stratification and regulatory performance, providing a foundation for optimizing system design and control strategies.

MODELING

Validation of the original CFD model

In a previous study [5], we encountered stratification issues in a water tank during the development of a soft sensor. Hot water (50 °C) was fed from the top side into a tank filled with cold water (10 °C) at a flow rate of 770 ml/min (or equivalent to 0.1889 m/s at the inlet), which exhibits complexity of natural and forced convections due to strong buoyant influences. Due to the similar main mechanisms existing in our following case study, this original case is suitable to examine our CFD settings. The solver buoyantPimpleFoam in OpenFOAM9 was adopted due to its capability to resolve transient thermo-hydrodynamics. The thermo-physical properties of water were assumed to be temperature-dependent, as described in reference [8], and the same formulations for density, heat conductivity, specific heat capacity, and viscosity were employed. The velocity of 0.1889 m/s was set at the inlet and the gauge pressure=0 Pa was set at the outlet.

Figure 1 (a) illustrates the original CFD model, which conforms to the experimental dimensions. Within the tank, the locations B1M (0.046 m, -0.046 m, 0.0635 m) and C3T (0 m, 0.092 m, 0.127 m) were monitored, consistent with reference [5] where temperature measurements were taken using thermocouples. For subsequent work, we also recorded temperature data from interior locations and a near-outlet sensor, making B1M and C3T suitable validation points. Hybrid mesh system is adopted, with 1.67 million grids in total. Hexa grids are dominant while unstructured grids are near the top to adapt inlet and outlet, as observed at the section X = -0.08 m. As shown in Figures 1(b) and (c), the CFD model results are consistent with experimental data.

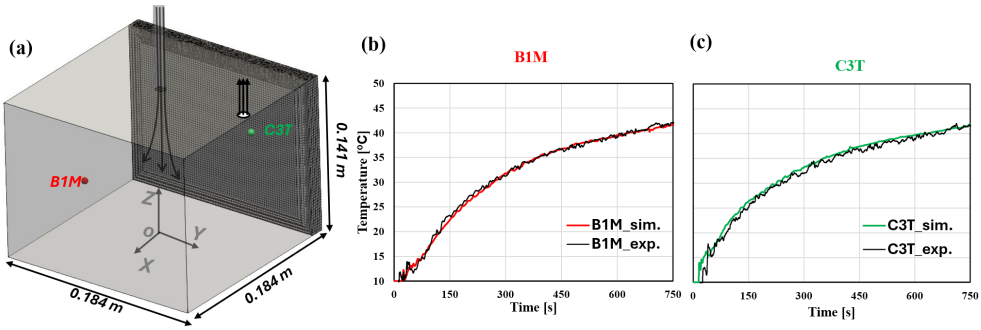

Figure 1. (a) The original CFD model used for validation, showing grid distribution at the section X = -0.08 m; temperature variations at (b) B1M and (c) C3T, comparing simulation results with experimental data.

Table 1. Case conditions

Case no.	1	2	3	4	5
Target (initial) temperature [°C]	25	20	45	20	20
Fed temperature [°C]	60	10	10	10	10
Ambient temperature [°C]	15	25	55	25	25
Drain nozzle (/sensor) location	top	top	top	Middle	bottom
Simulated time [s]	1200	1200	1200	1200	1800

The flow rate is always 770 ml/min (or 0.1889 m/s at the inlet)

Adaption and control system integration

The model was adapted by installing the inlet tube on the side of the tank, as shown in Figure 2(a). The inlet velocity and tank size were inherited from the validated CFD model (Figure 1(a)). Hexa-dominant hybrid grids are still adopted with unstructured ones constructed near the side with the inlet and outlet. Another interior location, B2M (0.046 m, 0.046 m, 0.0635 m), was added for temperature monitoring. Notably, three optional outlet positions (diameter = 9 mm) were considered, with center coordinates as follows: top (0 m, 0.078 m, 0.127 m), middle (0 m, 0.078 m, 0.014 m), and bottom (-0.078 m, 0.078 m, 0.0635 m). Corresponding near-outlet sensors (sensorT, sensorM, and sensorB) were positioned 0.014 m from the outlet centerline. When the outlet was at the top or bottom, only half of the domain was simulated using symmetric boundary conditions to save computational cost.

Table 1 summarizes all cases in this study, and Figure 2(b) illustrates the boundary conditions for Case 1 as an example. Unlike the adiabatic wall conditions in the original model (Figure 1(a)), all tank sides were simplified to imposed ambient temperatures, except for the bottom (representing the ground), to simulate environmental influences. The initial tank temperature was set to the target value in all cases. Cases 1 and 2 can be taken as typical regulation scenarios via heating and cooling in winter and summer, respectively. However, regulation issues were identified in Case 2, leading to the design of Cases 3-5 for further analysis. Except for Case 3, the target temperatures were set at 25 °C for heating and 20 °C for cooling.

The on-off control mechanism was implemented using programmable boundary conditions in OpenFOAM via codeStream. The inlet velocity was set to 0.1889 m/s ("On") or 0 m/s ("Off") based on feedback from the virtual sensor. In the heating scenario, the control mechanism was defined as follows:

$$\begin{cases} \boldsymbol{Off},\ T_{sen} \in (T_{targ}+1, +\infty) \\ \boldsymbol{Remain}\ on\ or\ off,\ T_{sen} \in [T_{targ}-1, T_{targ}+1] \\ \boldsymbol{On},\ T_{sen} \in (-\infty, T_{targ}-1) \end{cases} \quad (1)$$

where the T_{sen} represents the sensed temperature, and T_{targ} denotes the target temperature for regulation. In the cooling scenario, the mechanism was reversed, with "On" and "Off" conditions switched in Eq. (1). To account for control system delays in real-world applications, the acceptable temperature range was set to $[T_{targ}-1, T_{targ}+1]$. To illustrate the regulatory mechanism, an additional sensor (sensor0) was embedded to record velocity magnitude at the inlet tube connection, as depicted in Figure 2(b). The temperature at sensorT and the velocity at sensor0 are shown in Figure 2(c), with data after 600 s omitted for brevity due to repetitive patterns. To reach target temperature at sensorT, the water (60 °C) supply was turned off when the temperature at sensorT reached 26 °C and resumed when it dropped below 24 °C, corresponding to "Off" and "On" states, respectively.

RESULTS AND DISCUSSIONS

Temperature non-uniformity issue

Significant temperature non-uniformity was observed in Case 1. As shown in Figure 3(a) and (b), the

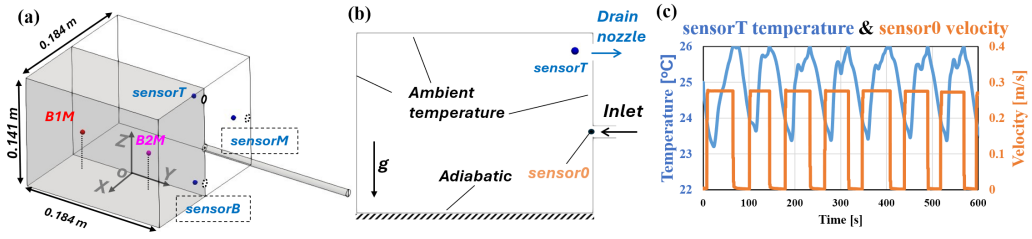

Figure 2. (a) Adapted CFD model with monitored points and optional outlet/sensor positions for case study; (b) I illustrations of boundary conditions; (c) the temperature at sensorT and velocity at sensor0 for Case 1.

temperatures at B1M and B2M began to oscillate steadily around certain levels after approximately 600 s. The calculated mean values between 600 s and 1200 s were 22.6 °C, 22.8 °C, and 24.9 °C at B1M, B2M, and sensorT, respectively. These results indicate temperature deviations at interior locations (B1M and B2M) of more than 2 °C from the target (25 °C), even though the control system maintained the sensor's temperature close to the target value. More seriously, as shown in Figure 3(c), at 835 s during the "on" state, temperatures below B1M and B2M were even lower, while some regions near the tank top exceeded 26 °C, further demonstrating stratification.

A more serious issue occurred in the cooling scenario (Case 2), where the regulatory mechanism operated abnormally due to the thermal stratification. As observed in Figure 4(a), the temperature at the sensor could not drop below the acceptable upper limit (21 ˚C) and failed to reach the off-triggering threshold (19 °C) throughout the simulation. Consequently, continuous cooling water feeding caused overcooling inside the tank. As shown in Figure 4(b), the mean temperature at B2M dropped to 17.9 ˚C after 900 s. Additionally, Figure 4(c) reveals that cooler regions persisted below B1M and B2M, indicating severe thermal non-uniformity.

Analyses on the regulation failure

Stratification in the cooling scenario was characterized by weak mixing effects, which disabled the regulatory mechanism. As shown in Figure 4(c), velocity vectors beneath B1M and B2M (highlighted in red frames) displayed swirling patterns, indicating the difficulty in transporting cold water into regions of retained hot water above. Some upward convection near the wall (black frame) was observed but was insufficient due to heating from ambient temperatures 25 °C imposed on the wall. Consequently, the thermal mixing was weak in Case 2, preventing the "off" state from being triggered.

Buoyancy was found to dominate stratification formation during thermal regulation. Figure 5(a) and (b) present temperature distributions at the central section (X = 0 m) during the "on" state for Cases 1 and 2, respectively. Buoyancy deflected the fed flow along its direction. In Case 3, which shared identical absolute temperature differences with Case 1 ($|T_{targ} - T_{fed}| = 35$ ˚C, $|T_{amb} - T_{fed}| = 45$ ˚C, T_{fed} and T_{amb} denote the fed and ambient temperatures, respectively), the stratification became more severe compared to Case 2. This ruled out temperature difference as the main factor for regulation failure and emphasized the stronger buoyant effects in Case 3, where greater density differences were present. Unfortunately, Case 3 also failed to trigger the "off" state. Buoyancy in Case 3 redirected the fed flow in the opposite direction of the outlet, contributing to stratification.

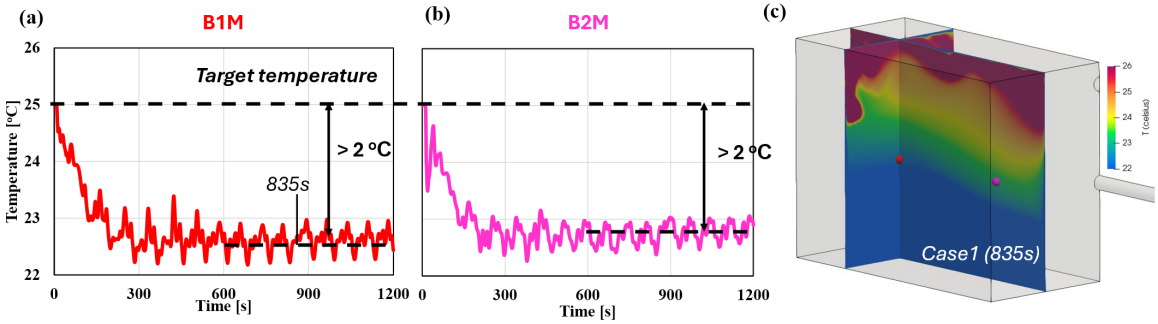

Figure 3. Case 1 results: temperature variations at (a) B1M and (b) B2M; (c) temperature contour at 835 s.

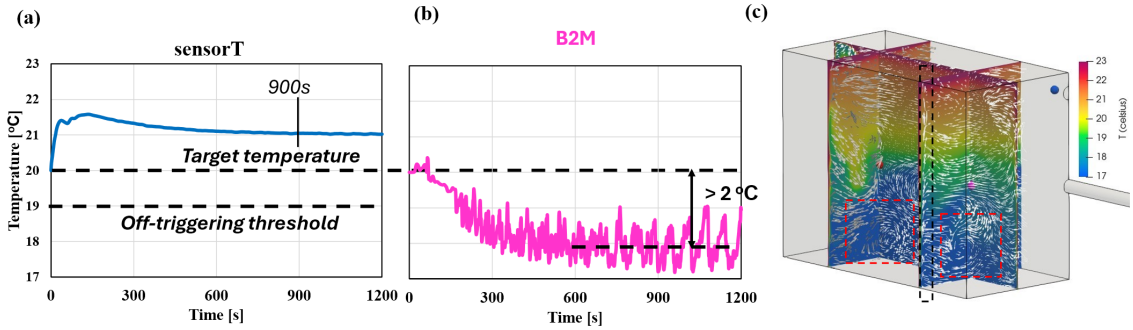

Figure 4. Case 2 results: temperature variations at (a) sensorT and (b) B2M; (C) temperature contour with velocity vectors at 900 s.

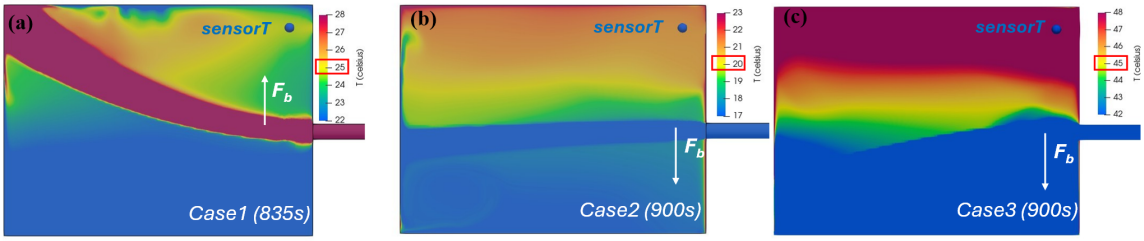

Figure 5. Temperature contours at the tank center (section at X = 0 m) for (a) Case 1 (835s) (b) Case 2 at 900 s and (c) Case 3 at 900 s. Framed values on legend indicate target temperatures for corresponding cases.

In contrast, buoyancy in Case 1 aided regulation by pushing fed water toward the outlet, enabling the sensor to detect variations effectively.

Influences of the outlet position

To activate the "off" state, outlet positions and their corresponding sensors were varied. Cases 4 and 5, sharing identical initial, target, fed, and ambient temperatures with Case 2, positioned outlets in the middle and bottom of the tank, respectively. Notably, Case 4 required simulating the entire domain, unlike the half-domain simulations in other cases, due to symmetry breaking. As shown in Figure 6(a), the middle outlet in Case 4 failed to trigger the "off" state, with sensorM temperatures remaining above 19 ˚C even after 1200 s elapsed. In contrast, Case 5 successfully activated the on-off mechanism (see Figure 6 (d)), but its oscillation cycles (average more than 200 s) were longer than those in Case 2 (average less than 100 s). The simulation for Case 5 was extended to 1800 s to capture steady oscillation patterns while conserving computational resources.

Varying the outlet position cannot eliminate stratification, but it can alleviate non-uniformity severity. As demonstrated in Figure 6 (c), the stratification still exists in Case 4, although temperatures at B2M is nearly stable at the target level (see Figure 6 (b)). In Case 5, despite the mean temperature value at sensorB (Figure 6 (d)) is 20.1 °C between 900 s and 1800 s, the B2M's mean value is 22.1 °C, 2 °C higher than the target level (Figure 6 (e)). Among Cases 2, 4, and 5 (Figure 4(c), Figure 6(c), and Figure 6(f)), the top outlet in Case 2 resulted in the least severe stratification, while Case 5 showed the worst distribution, with over half the regions exceeding 22 °C (Figure 6(f)), despite normal regulatory operation. This can be attributed to the higher-temperature water being retained at higher locations, making it easier to discharge through a top outlet. Conversely, fed cold water tended

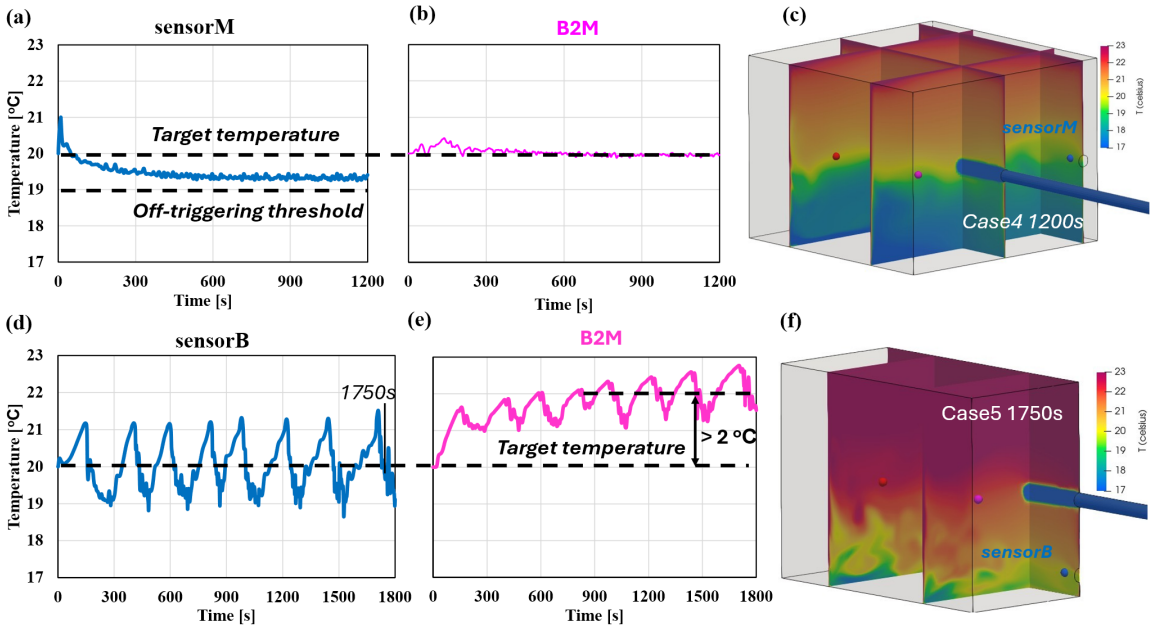

Figure 6. Temperature variations in Case 4 at (a) sensorM and (b) B2M; (c) temperature contour of Case 4 at 1200 s; Temperature variations of Case 5 at (d) sensorM and (e) B2M; (f) temperature contour of Case 5 at 1750 s.

to accumulate at lower locations, facilitating its exhaustion through a bottom outlet. Therefore, it is advisable to position the outlet on the side opposite to the buoyancy direction, while the resolving of regulation failure should resort to other strategies except for outlet positions.

Modifications in future work

In summary, the temperature regulations in this study faced challenges due to stratification and abnormal operations. The single input fluid combined with an on-off control mechanism failed to achieve uniform temperature distribution at the target level. Future strategies can consider adding internal circulation procedure in the regulation mechanism (e.g., the thermo-on/off control in air-conditioning) or using our proposed dual-input systems [9]. Previous research on soft sensors may also provide solutions, particularly given the difficulties in increasing the number of internal sensors [4,5].

CONCLUSIONS

A CFD-based temperature regulation model for a liquid tank was developed by adapting a validated CFD model. An on-off control mechanism was integrated with $\pm$ 1 °C relative to the target temperature as the acceptable limits. Both heating and cooling regulating scenarios were simulated to investigate the temperature non-uniformity inside the tank. The following conclusions were drawn: (1)buoyancy can induce thermal stratification, leading to interior temperature discrepancies exceeding the acceptable range relative to the target value; (2) thermal stratification can even disable the regulatory mechanism in cooling scenarios, as the conventional near-outlet sensor fails to drop below the "off" triggering threshold (acceptable lower limit) ; (3) Positioning the outlet on the side opposite to the buoyancy direction can mitigate (but not eliminate) thermal non-uniformity by facilitating the removal of retained water.

In summary, our virtual CFD model can provide detailed thermal field information during liquid temperature regulation, offering a controlled environment to explore the system improvement without experimental constraints. The insights gained from the thermal field analysis can guide the development of more effective temperature regulation designs and strategies.

ACKNOWLEDGEMENTS

This research is financially supported by New Energy and Industrial Technology Development Organization (NEDO), JPNP20004, Japan.

The authors thank the Supercomputer Center, the Institute for Solid State Physics, the University of Tokyo for the use of the facilities.

REFERENCES

1. Caravella A, Francardi M, Romano S, Prenesti G, Oliverio M. Optimization of temperature distribution in the novel power-to-heat matrix-in-batch OnePot© reactor. *Front. Energy Res.* 10: 964511 (2022)
2. Xu L, Su J, Chen H, Ye J, Qin K, Zhang W, Yang Y, Zhu H. Continuous-flow microwave heating system with high efficiency and uniformity for liquid food. *Innov. Food Sci. Emerg. Technol.* 91: 103556 2024
3. Taler D, Sobota T, Jaremkiewicz M, Taler J. Control of the temperature in the hot liquid tank by using a digital PID controller considering the random errors of the thermometer indications. *Energy* 239: 122771 (2022)
4. Xu F, Sakurai K, Sato Y, Sakai Y, Sabu S, Kanayama H, Satou D, Kansha Y. Soft-Sensor Modeling of Temperature Variation in a Room under Cooling Conditions. *Energies* 16: 2870 (2023)
5. Xu F, Wang J, Sakurai K, Sakai Y, Sabu S, Kanayama H, Zhang R, Satou D, Kansha Y. Soft-sensor model for indoor temperature prediction under heating conditions. *Therm. Sci. Eng. Prog.* 51: 102650 (2024)
6. Sun Z, Wang S. A CFD-based test method for control of indoor environment and space ventilation. *Build. Environ.* 45: 1441–7 2010
7. Sun Y, Zhang Y, Guo D, Zhang X, Lai Y, Luo D. Intelligent Distributed Temperature and Humidity Control Mechanism for Uniformity and Precision in the Indoor Environment. *IEEE Internet Things J.* 9: 19101–15 (2022)
8. Lou W, Baudin N, Roux S, Fan Y, Luo L. Impact of buoyant jet entrainment on the thermocline behavior in a single-medium thermal energy storage tank. *J. Energy Storage* 71: 108017 (2023)
9. Wang Jinxin, Xu Feng, Sakurai Kei, Sakai Yuka, Sabu Shunsuke, Zhang Ruizi, Kanayama Hiroaki, Satou Daisuke, Kansha Yasuki. Investigation of Fluid Dynamics in the Case of Two Higher-temperature Fluid Inputs to Effectively Heat the Vessels *Chem. Eng. Trans.* 114: 271–6 (2024)